Published in final edited form as:

Chem Commun (Camb). 2019 September 28; 55(76): 11402–11405. doi:10.1039/c9cc06239d.

Tailoring the pore geometry and chemistry in microporous metal–organic frameworks for high methane storage working capacity†

Kai Shao[a], **Jiyan Pei**[a], **Jia-Xin Wang**[a], **Yu Yang**[a], **Yuanjing Cui**[a], **Wei Zhou**[b], **Taner Yildirim**[b], **Bin Li**[a,*], **Banglin Chen**[c], **Guodong Qian**[a,*]

[a]State Key Laboratory of Silicon Materials, Cyrus Tang Center for Sensor Materials and Applications, Department of Materials Science & Engineering, Zhejiang University, Hangzhou 310027, China.

[b]NIST Center for Neutron Research, National Institute of Standards and Technology, Gaithersburg, Maryland 20899-6102, USA

[c]Department of Chemistry, University of Texas at San Antonio, One UTSA Circle, San Antonio, Texas 78249-0698, USA.

Abstract

We realized that tailoring the pore size/geometry and chemistry, by virtue of alkynyl or naphthalene replacing phenyl within a series of isomorphic MOFs, can optimize methane storage working capacities, affording an exceptionally high working capacity of 203 cm^3 (STP) cm^{-3} at 298 K and 5–80 bar.

The exponential increase in global energy usage over the past 50 years has pushed the implementation of a cleaner fuel for replacing conventional petroleum fuels to a level of utmost importance. Natural gas (NG), primarily composed of methane, holds bright promise as a viable alternative fuel due to its abundant reserves, low CO_2 emission and high research octane number (RON = 107). However, its widespread use is limited by the relatively low volumetric energy density. Although liquefied NG (LNG) at 113 K and compressed NG (CNG) at 250 bar are already in use, cryogenic and high-pressure storage conditions have severely hampered practical applications. For instance, overhigh pressures required for liquefaction can only be achieved by using complex and expensive multi-stage compressors, leading to some cost, space, and safety issues for use in passenger vehicles. In this regard, adsorbed natural gas (ANG) systems have aroused considerable interest to overcome these issues, which involves filling storage tanks with porous materials to store a high density of methane at modest pressures. To guide the research of the ANG technology, the U.S.

†Electronic supplementary information (ESI) available: Synthesis, PXRD, sorption data, NMR, optical images and structural data for PCN-46 and ZJU-105. CCDC 1943325. For ESI and crystallographic data in CIF or other electronic format see DOI: 10.1039/c9cc06239d

* bin.li@zju.edu.cn, gdqian@zju.edu.cn, Fax: +1-210-458-7428.

Conflicts of interest

There are no conflicts to declare.

Department of Energy (DOE) has set the ambitious volumetric NG storage target of 263 cm^3 (STP) cm^{-3} at room temperature (RT) assuming the adsorbent packing loss is ignored, equivalent to that of CNG at 250 bar and 298 K.[1]

Extensive research efforts have been devoted to developing new materials with high methane storage capacity in order to meet the challenging storage target. Microporous metal–organic frameworks (MOFs) are known to be very promising for methane storage because of their high surface areas, tunable pores, and versatile chemistry.[2–4] A large number of MOFs, such as HKUST-1, UTSA-76, Co(BDP), MOF-5, NU-125, Al-soc-MOF-1, MAF-38, MOF-905, NJU-Bai43, and MFM-115 have been reported as outstanding storage adsorbents, showing some of the highest gravimetric or volumetric CH_4 storage capacities.[5–11] It is notable that the volumetric working capacity is a key parameter to evaluate the performance of methane storage materials, because it determines the driving range of vehicles powered by natural gas. Since the automobile industry requires an engine inlet pressure of 5 bar, the working capacity (also called deliverable capacity) is defined as the difference of the amount of methane adsorbed between the target storage pressure (generally 35–80 bar) and 5 bar. Prominently, there are two pathways to improve the methane working capacity of a given porous material. On one hand, optimizing pore sizes or functional sites in MOFs can enforce the strength of host–methane and methane–methane interactions (Q_{st}), contributing to high volumetric methane uptake at high pressure.[5,6] Nevertheless, overhigh Q_{st} in MOFs leads to a rapid increase in the low-pressure uptake, sometimes delimiting their high working capacity, as exemplified by MOF-74 and PCN-14.[6] On the other hand, large-pore MOFs (*e.g.*, MOF-905, Al-soc-MOF-1 and NU-111) commonly show moderate Q_{st} for methane, resulting in a low CH_4 adsorption at 5 bar;[9,10] however, too weak CH_4 affinity delimits the total CH_4 uptake at high pressure, thus sacrificing the working capacity in some cases.[10] Evidently, it is highly desired to optimize the porous structures with suitable methane binding affinity for balancing the CH_4 adsorption amounts between the high and low pressure, thus targeting higher volumetric working capacity.

With this in mind, we herein used a crystal-engineering strategy to finely modulate the pore size and chemistry in a family of isomorphic MOFs for methane storage. We chose NOTT-102 as the fundamental framework backbone because of its high methane storage capacity and easily adjustable functionality on the center phenyl rings.[14] The use of alkynyl or naphthalene groups to replace the phenyl rings in NOTT-102 afforded two porous materials (namely PCN-46 and ZJU-105), in which the pore size and pore-chemistry can be well modulated (Fig. 1). It was found that the expanded pore size and reduced aromatic CH_4-affinity sites in PCN-46a can cause a slight decrease in the low-pressure CH_4 uptake while having a negligible effect on the adsorption at 65/80 bar, leading to an exceptionally high volumetric working capacity of 203 cm^3 (STP) cm^{-3} between 5 and 80 bar at 298 K. This value is comparable to the best-performing MOFs reported, such as MFM-115a (208 cm^3 (STP) cm^{-3})[12] and MOF-905 (203 cm^3 (STP) cm^{-3}).[13]

The linkers of H_4L1 and H_4L2 were elaborately designed by using two naphthalene or alkynyl groups replacing the phenyl rings on the linker of NOTT-102 (Fig. 1). Both of the organic linkers were synthesized through a multistep reaction procedure (Schemes S1 and S2, ESI†). A solvothermal reaction of H_4L1 with $Cu(NO_3)_2{\cdot}2.5H_2O$ in a mixture of

DMF/H_2O (in the presence of HCl) at 80 °C for 3 days afforded blue block crystals of a novel MOF (ZJU-105) with a framework formula of $[Cu_2(L1)(H_2O)_2]_n$. High-quality crystals of PCN-46, $[Cu_2(L2)(H_2O)_2]_n$, were synthesized by a solvothermal reaction of H_4L2 with $Cu(NO_3)_2{\cdot}2.5H_2O$ in a mixture of DMF/EtOH/H_2O (in the presence of HNO_3) at 85 °C for 1 day. It is worth noting that the sample of PCN-46 in the literature was directly synthesized by using a precursor compound (5-ethynylisophthalic acid) of H_4L2 to react with copper salts, which cannot guarantee the high quality of the bulk samples.[15] In this work, the phase purity of bulk materials for ZJU-105 and PCN-46 was confirmed by powder X-ray diffraction (PXRD) and the following surface area/pore volume measured (Fig. S10–S15, ESI†).

The crystal structures of the three MOFs investigated are schematically shown in Fig. 1. Structural analysis reveals that both of the ZJU-105 and PCN-46 frameworks are isoreticular to NOTT-102, which consist of paddle-wheel dinuclear $Cu_2(COO)_4$ units linked by the carboxylates of L^{4-} linkers to form a 3D NbO-type network.[14d] As expected, the use of alkynyl or naphthalene groups to replace the phenyl rings on NOTT-102 can finely modulate the pore size/geometry and chemistry. As shown in Fig. 1, the framework of NOTT-102 has two types of cages: one cuboctahedral cage of about 12.5 × 14.7 $Å^2$ and another large irregular elongated cage of ≈9.6 × 28.6 $Å^2$. When the bulky naphthalene rings were incorporated, the pores of ZJU-105 were significantly decreased, wherein the large irregular cage was divided into three small cages with the diameters of 3.8 and 8.0 Å. In contrast, we slim down the organic ligands in PCN-46 by virtue of triple-bond spacers replacing the phenyls in NOTT-102. Relative to NOTT-102, PCN-46 exhibits a similar pore geometry with slightly expanded pore spaces. In addition, the incorporation of alkynyl or naphthalene groups in PCN-46 and ZJU-105 can reduce or increase the aromatic moieties that provide $\pi\cdots CH_4$ interactions.[16] Therefore, the fine-tuned pore size/geometry and aromatic moieties in this series of MOFs can systematically affect the strength of CH_4 binding affinities, thus optimizing the target working capacities.

Before methane adsorption measurements, we first measured the N_2 adsorption isotherms at 77 K of the activated ZJU-105a and PCN-46a. As shown in Fig. 2a, the N_2 isotherms of ZJU-105a and PCN-46a exhibit a reversible type-I character with saturated uptake of 670 and 803 $cm^3\ g^{-1}$, respectively. The Brunauer–Emmett–Teller (BET) surface area and pore volume of ZJU-105a were determined to be 2608 $m^2\ g^{-1}$ and 1.037 $cm^3\ g^{-1}$, respectively, notably lower than those of NOTT-102a (3342 $m^2\ g^{-1}$ and 1.268 $cm^3\ g^{-1}$) due to the incorporated bulky naphthalene groups. In contrast, PCN-46a with the slimmed alkynyl groups shows a comparable BET surface area and pore volume (3224 $m^2\ g^{-1}$ and 1.243 $cm^3\ g^{-1}$). We note that these values of PCN-46a are significantly higher than the reported values (2500 $m^2\ g^{-1}$ and 1.012 $cm^3\ g^{-1}$) in the previous literature,[15] and agree well with the theoretical ones (3634 $m^2\ g^{-1}$ and 1.266 $cm^3\ g^{-1}$) calculated from the crystal structure. This further confirms the high quality of the bulk samples that we synthesized, encouraging us to retest their methane storage capacities.

Next, we collected the high-pressure methane adsorption isotherms for ZJU-105a and PCN-46a at 273 and 298 K over the pressure range of 0–100 bar. As presented in Fig. 2b and c, ZJU-105a and PCN-46a exhibit high total volumetric methane uptake values of 228 and

233 cm^3 (STP) cm^{-3} at 65 bar and 298 K, respectively. These values are comparable to that of NOTT-102a (233 cm^3 (STP) cm^{-3}), indicating that tuning the pore size/geometry in these isomorphic MOFs shows a negligible effect on the total volumetric CH_4 uptake at high pressure. This might be attributed to the mutual compensation between the porosity, crystal density and CH_4 binding strength. With the pressure increasing to 80 bar, the volumetric uptake of ZJU-105a and PCN-46a can be further increased to 243 and 246 cm^3 (STP) cm^{-3}, respectively, achieving 93% of the new DOE's volumetric target assuming the packing density loss is ignored. These values are higher than those of most of the promising MOFs, such as MOF-905 (228 cm^3 (STP) cm^{-3})[13] and Al-soc-MOF-1 (221 cm^3 (STP) cm^{-3}),[9a] and approach those of the best-performing MFM-115 (256 cm^3 (STP) cm^{-3})[12] and HKUST-1 (272 cm^3 (STP) cm^{-3}).[4b]

In practical applications, the driving range of an ANG vehicle is determined primarily by the working capacity of the adsorbent. We first evaluated the volumetric working capacities of ZJU-105a and PCN-46a to compare with NOTT-102a and some other indicated MOFs (Table 1). As shown in Fig. 2d, due to the smaller pore spaces and more aromatic moieties, ZJU-105a takes up more CH_4 (53 cm^3 (STP) cm^{-3}) at 5 bar than NOTT-102a (48 cm^3 (STP) cm^{-3}). In contrast, PCN-46a shows a lower adsorption at 5 bar (43 cm^3 (STP) cm^{-3}) than NOTT-102a. Therefore, PCN-46a exhibits a higher volumetric working capacity of 190 cm^3 (STP) cm^{-3} than NOTT-102a (185 cm^3 (STP) cm^{-3}) and ZJU-105a (175 cm^3 (STP) cm^{-3}) between 65 and 5 bar at 298 K. It is worth noting that this working capacity of PCN-46a outperforms that of most of the promising MOFs (*e.g.,* NU-125, NU-111, UTSA-20, Al-soc-MOF-1, and MOF-5, Table 1), and is comparable to that of the benchmark HKUST-1 (190 cm^3 (STP) cm^{-3}),[4a] MFM-115 (191 cm^3 (STP) cm^{-3}),[12] and UTSA-76a (197 cm^3 (STP) cm^{-3}).[11] When the storage pressure is increased to 80 bar, PCN-46a exhibits an exceptionally high CH_4 working capacity of 203 cm^3 (STP) cm^{-3} between 80 and 5 bar at RT (Fig. 3), much higher than that of ZJU-105a (190 cm^3 (STP) cm^{-3}) and rivaling the state-of-the-art materials reported, such as MFM-115a (208 cm^3 (STP) cm^{-3})[12] and MOF-905 (203 cm^3 (STP) cm^{-3}).[13]

To gain better insight into the origin of different volumetric low-pressure uptake values and working capacities of ZJU-105a and PCN-46a, we first calculated their isosteric heats of adsorption (Q_{st}) from the temperature-dependent isotherms using the virial method (Fig. S22–S24, ESI†). The initial Q_{st} of ZJU-105a was calculated to be 16.58 kJ mol^{-1}, much higher than those of NOTT-102a (14.90 kJ mol^{-1}) and PCN-46a (14.2 kJ mol^{-1}). Due to the same framework backbone and topology, these MOFs have a similar density of open metal sites. The incorporation of naphthalene groups in ZJU-105a can not only notably reduce the pore sizes but also offer more aromatic moieties to interact with CH_4 molecules *via* $\pi\cdots CH_4$ interactions,[16] contributing to the enhanced CH_4 affinity and thus a higher CH_4 adsorption at low pressure of 5 bar than that of NOTT-102a. In contrast, the use of alkynyl groups to replace the benzene rings in PCN-46a can slightly expand the pore sizes with no aromatic moieties, resulting in lower CH_4 affinity and uptake at 5 bar. Therefore, PCN-46a shows the lowest low-pressure CH_4 uptake among these three MOFs, thus affording the highest volumetric working capacity.

We have also studied the CO_2 and H_2 uptake properties of ZJU-105a and PCN-46a over wide temperature and pressure ranges (Fig. S18–S21, ESI†). ZJU-105a and PCN-46a exhibit high total volumetric H_2 storage capacities of 48 g L^{-1} (6.78 wt%) and 50 g L^{-1} (7.47 wt%) at 65 bar and 77 K, meeting the DOE's targets of 40 g L^{-1} (5.5 wt%), albeit at 77 K rather than at ambient temperature. These volumetric values are comparable to those of some of the benchmark MOFs (Table S4, ESI†). The volumetric and gravimetric working capacities of PCN-46a, calculated from (T_{min} = 77 K, P_{max} = 65 bar) to (T_{max} = 160 K, P_{min} = 5 bar), are 47.4 g L^{-1} and 7.1 wt%, rivaling the best-performing material IRMOF-20 (47 g L^{-1} and 8.4 wt%).[17] In addition, ZJU-105a and PCN-46a also exhibit high volumetric CO_2 storage capacities of 328 and 309 cm^3 (STP) cm^{-3} (Table S5, ESI†). Finally, we calculated the Q_{st} values of H_2 and CO_2 for both MOFs. As shown in Fig. S25–S30 (ESI†), the Q_{st} values of ZJU-105a for both H_2 and CO_2 are much higher than those of PCN-46a, consistent with those for CH_4, further confirming that PCN-46a has a weaker interaction with various gas molecules.

In summary, we herein realized that the systematical tuning of the pore size and chemistry in a series of isomorphic MOFs based on NOTT-102 can effectively regulate the methane storage and working capacities. The use of alkynyl and naphthalene replacing phenyl in the NOTT-102 backbone has enabled a gradually decreased low-pressure CH_4 uptake from ZJU-105a to PCN-46a, combined with a comparable total storage capacity at high pressure. PCN-46a thus exhibits the highest working capacity of 203 cm^3 (STP) cm^{-3} (at 5–80 bar and 298 K) among the isomorphic MOFs, making it among the best performing porous materials for CH_4 storage. This work may provide some guidance for the development of new MOFs with common alkynyl connectivity instead of phenyl to reduce low-pressure CH_4 absorption and thus to improve the volumetric working capacity.

Supplementary Material

Refer to Web version on PubMed Central for supplementary material.

Acknowledgments

This research was supported by the "National 1000 Young Talent Program", the "Zhejiang University 100 Talent Program", and the National Natural Science Foundation of China (51803179).

Notes and references

1. He Y, Zhou W, Qian G and Chen B, Chem. Soc. Rev, 2014, 43, 5657. [PubMed: 24658531]
2. (a)Furukawa H, Cordova KE, O'Keeffe M and Yaghi OM, Science, 2013, 341, 1230444;(b)Li B, Wen H-M, Cui Y, Zhou W, Qian G and Chen B, Adv. Mater, 2016, 28, 8819. [PubMed: 27454668]
3. (a)Wang H and Li J, Acc. Chem. Res, 2019, 52, 1968; [PubMed: 30883088] (b)Nugent P, Belmabkhout Y, Burd SD, Cairns AJ, Luebke R, Forrest K, Pham T, Ma S, Space B, Wojtas L, Eddaoudi M and Zaworotko M, Nature, 2013, 495, 80; [PubMed: 23446349] (c)Wang H, Zhu Q-L and Xu Q, Chem, 2017, 2, 52;(d)Li B, Wen H-M, Yu Y, Cui Y, Zhou W, Chen B and Qian G, Mater. Today Nano, 2018, 2, 21;(e)Wen H-M, Liao C, Li L, Wu H, Zhou W, Hu J and Chen B, J. Mater. Chem. A, 2019, 7, 3128.
4. (a)Peng Y, Krungleviciute V, Eryazici I, Hupp JT, Farha OK and Yildirim T, J. Am. Chem. Soc, 2013, 135, 11887;(b)Mason JA, Veenstra M and Long JR, Chem. Sci, 2014, 5, 32;(c)Makal TA, Li

J-R, Lu W and Zhou H-C, Chem. Soc. Rev, 2012, 41, 7761; [PubMed: 22990753] (d)Li B, Wen H-M, Zhou W, Xu JQ and Chen B, Chem, 2016, 1, 557.

5. (a)Hulvey Z, Vlaisavljevich B, Mason JA, Tsivion E, Dougherty TP, Bloch ED, Head-Gordon M, Smit B, Long JR and Brown CM, J. Am. Chem. Soc, 2015, 137, 10816;(b)Chen C-X, Wei Z-W, Jiang J-J, Zheng S-P, Wang H-P, Qiu Q-F, Cao C-C, Fenske D and Su C-Y, J. Am. Chem. Soc, 2017, 139, 6034; [PubMed: 28388035] (c)Zhang M, Zhou W, Pham T, Forrest KA, Liu W, He Y, Wu H, Yildirim T, Chen B, Space B, Pan Y, Zaworotko MJ and Bai J, Angew. Chem., Int. Ed, 2017, 56, 11426.
6. (a)Wu H, Zhou W and Yildirim T, J. Am. Chem. Soc, 2009, 131, 4995; [PubMed: 19275154] (b)Ma S, Sun D, Simmons JM, Collier CD, Yuan D and Zhou H-C, J. Am. Chem. Soc, 2008, 130, 1012. [PubMed: 18163628]
7. (a)Liang C-C, Shi Z-L, He C-T, Tan J, Zhou H-D, Zhou H-L, Lee Y and Zhang Y-B, J. Am. Chem. Soc, 2017, 139, 13300;(b)Tran LD, Feldblyum JI, Wong-Foy AG and Matzger AJ, Langmuir, 2015, 31, 2211; [PubMed: 25621891] (c)Li L, Bell JG, Tang S, Lv X, Wang C, Xing Y, Zhao X and Thomas KM, Chem. Mater, 2014, 26, 4679;(d)Tian T, Zeng Z, Vulpe D, Casco ME, Divitini G, Midgley PA, Silvestre-Albero J, Tan JC, Moghadam PZ and Fairen-Jimenez D, Nat. Mater, 2018, 17, 174. [PubMed: 29251723]
8. (a)Mason JA, Oktawiec J, Taylor MK, Hudson MR, Rodriguez J, Bachman JE, Gonzalez MI, Cervellino A, Guagliardi A, Brown CM, Llewellyn PL, Masciocchi N and Long JR, Nature, 2015, 527, 357; [PubMed: 26503057] (b)Yang Q-Y, Lama P, Sen S, Lusi M, Chen KJ, Gao W-Y, Shivanna M, Pham T, Hosono N, Kusaka S, Perry J. J. t., Ma S, Space B, Barbour LJ, Kitagawa S and Zaworotko MJ, Angew. Chem., Int. Ed, 2018, 57, 5684;(c)Kundu T, Shah BB, Bolinois L and Zhao D, Chem. Mater, 2019, 31, 2842.
9. (a)Alezi D, Belmabkhout Y, Suyetin M, Bhatt PM, Weseliński J, Solovyeva V, Adil K, Spanopoulos I, Trikalitis PN, Emwas A-H and Eddaoudi M, J. Am. Chem. Soc, 2015, 137, 13308;(b)Tu B, Diestel L, Shi Z-L, Bandara WRLN, Chen Y, Lin W, Zhang Y-B, Telfer SG and Li Q, Angew. Chem., Int. Ed, 2019, 131, 5402;(c)Wilmer CE, Farha OK, Yildirim T, Eryazici I, Krungleviciute V, Sarjeant AA, Snurr RQ and Hupp JT, Energy Environ. Sci, 2013, 6, 1158.
10. (a)Gándara F, Furukawa H, Lee S and Yaghi OM, J. Am. Chem. Soc, 2014, 136, 5271; [PubMed: 24661065] (b)Peng Y, Srinivas G, Wilmer CE, Eryazici I, Snurr RQ, Hupp JT, Yildirim T and Farha OK, Chem. Commun, 2013, 49, 2992;(c)Yuan D, Zhao D, Sun D and Zhou H-C, Angew. Chem., Int. Ed, 2010, 49, 5357.
11. Li B, Wen H-M, Wang H, Wu H, Tyagi M, Yildirim T, Zhou W and Chen B, J. Am. Chem. Soc, 2014, 136, 6207. [PubMed: 24730649]
12. Yan Y, Kolokolov DI, Silva I. d., Stepanov AG, Blake AJ, Dailly A, Manuel P, Tang CC, Yang S and Schröder M, J. Am. Chem. Soc, 2017, 139, 13349.
13. Jiang J, Furukawa H, Zhang Y-B and Yaghi OM, J. Am. Chem. Soc, 2016, 138, 10244.
14. (a)Wen H-M, Li B, Li L, Lin R-B, Zhou W, Qian G and Chen B, Adv. Mater, 2018, 30, 1704792; (b)He Y, Zhou W, Yildirim T and Chen B, Energy Environ. Sci, 2013, 6, 2735;(c)Yan Y, Juricek M, Coudert FX, Vermeulen NA, Grunder S, Dailly A, Lewis W, Blake AJ, Stoddart JF and Schröder M, J. Am. Chem. Soc, 2016, 138, 3371; [PubMed: 26928460] (d)Lin X, Telepeni I, Blake AJ, Dailly A, Brown CM, Simmons JM, Zoppi M, Walker GS, Thomas KM, Mays TJ, Hubberstey P, Champness NR and Schröder M, J. Am. Chem. Soc, 2009, 131, 2159. [PubMed: 19159298]
15. Zhao D, Yuan D, Yakovenko A and Zhou H-C, Chem. Commun, 2010, 46, 4196.
16. (a)Lin J-M, He C-T, Liu Y, Liao P-Q, Zhou D-D, Zhang J-P and Chen X-M, Angew. Chem., Int. Ed, 2016, 55, 4752;(b)Spanopoulos I, Tsangarakis C, Klontzas E, Tylianakis E, Froudakis G, Adil K, Belmabkhout Y, Eddaoudi M and Trikalitis PN, J. Am. Chem. Soc, 2016, 138, 1568; [PubMed: 26694977] (c)Wu H, Simmons JM, Liu Y, Brown CM, Wang X-S, Ma S, Peterson VK, Southon PD, Kepert CJ, Zhou H-C, Yildirim T and Zhou W, Chem. – Eur. J, 2010, 16, 5205. [PubMed: 20358553]
17. Ahmed A, Liu Y, Purewal J, Tran LD, Wong-Foy AG, Veenstra M, Matzger AJ and Siegel DJ, Energy Environ. Sci, 2017, 10, 2459.

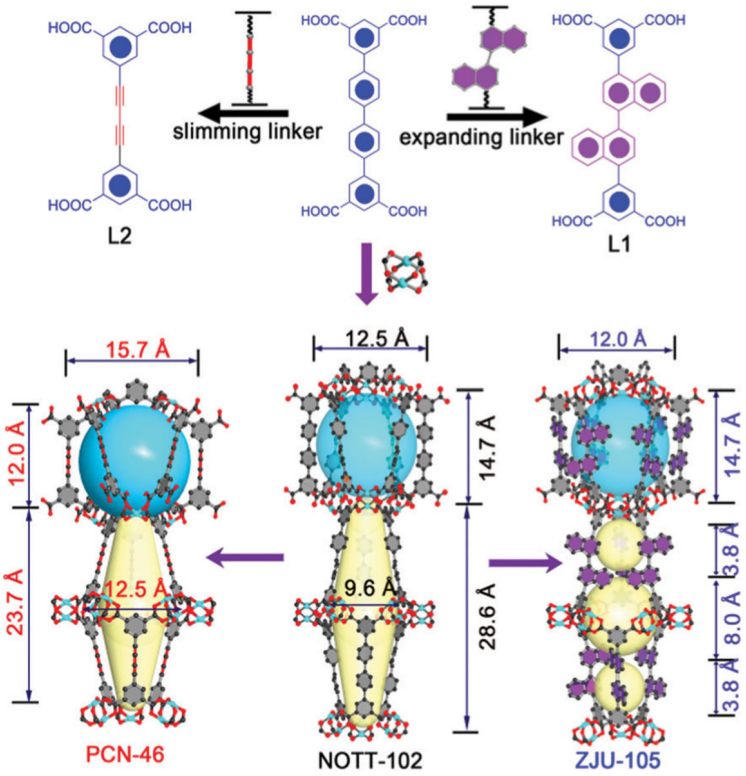

Fig. 1.

Comparison of the organic linkers and crystal structures of ZJU-105, NOTT-102, and PCN-46.

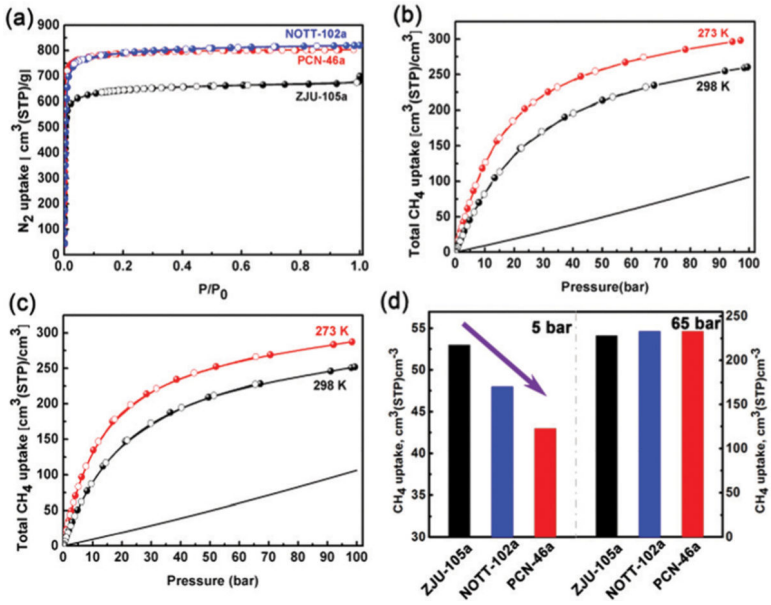

Fig. 2.

(a) Nitrogen isotherms of ZJU-105a, NOTT-102a and PCN-46a at 77 K. (b) Total volumetric CH_4 adsorption isotherms of PCN-46a and (c) ZJU-105a. (d) Comparison of the CH_4 adsorption amount of the indicated MOFs at 5 and 65 bar.

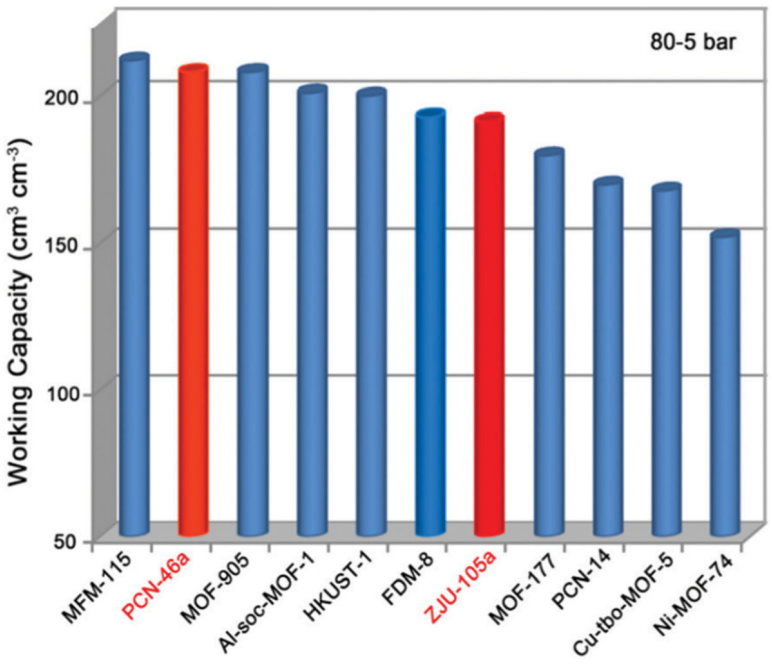

Fig. 3.

Comparison of the volumetric CH_4 working capacities of PCN-46a and ZJU-105a with some best-performing MOFs reported at 298 K.

Table 1

Summary of some promising MOFs for high-pressure CH_4 storage

MOFs	S_{BET} [a] ($m^2\ g^{-1}$)	Total uptake [b] cm^3/cm^3	Working capacity [c] cm^3/cm^3	Q_{st} (kJ mol^{-1})
PCN-46a	3224	246 (233)	203 (190)	14.2
ZJU-105a	2608	243 (228)	190 (175)	16.58
MFM-115a[12]	3394	256 (238)	208 (191)	16.3
MOF-905[13]	3490	228 (206)	203 (181)	11.7
NOTT-102a[14a]	3342	−(233)	−(185)	14.90
Al-soc-MOF-1[9a]	5585	221 (197)	201 (176)	11.0
HKUST-1[4a,b]	1850	272 (267)	200 (190)	17.0
UTSA-76[11]	2820	−(257)	−(197)	15.5
MAF-38[16a]	2022	273 (263)	197 (187)	21.6
FDM-8[9b]	3643	215 (193)	193 (171)	10.4
MOF-177[10a]	4500	205 (187)	185 (167)	9.9
NU-125[4a]	3120	−(232)	−(183)	15.1
PCN-14[4a,b]	2000	250 (230)	178 (157)	18.7
Cu-tbo-MOF-5[16b]	3971	216 (199)	175 (158)	20.4
Ni-MOF-74[4a,b]	1350	267 (251)	152 (129)	21.4

[a] Calculated from N_2 isotherms at 77 K.

[b] At 80(65) bar and 298 K.

[c] The working capacity is defined as the difference in the total uptake values between 80(65) and 5 bar.